N89-15955

GOES DYNAMIC PROPAGATION OF ATTITUDE

F. Landis Markley and Ed Seidewitz, Goddard Space Flight Center

Don Chu and John N. Rowe, Computer Sciences Corporation

ABSTRACT

The spacecraft in the next series of Geostationary Operational Environmental Satellites (GOES-Next) are Earth pointing and have 5-year mission lifetimes. Because gyros can be depended on only for a few years of continuous use, they will be turned off during routine operations. This means attitude must, at times, be determined without benefit of gyros and, often, using only Earth sensor data. To minimize the interruption caused by dumping angular momentum, these spacecraft have been designed to reduce the environmental torque acting on them and incorporate an adjustable solar trim tab for fine adjustment. A new support requirement for GOES-Next is that of setting the solar trim tab. Optimizing its setting requires an estimate of the unbalanced torque on the spacecraft. These two requirements, determining attitude without gyros and estimating the external torque, are addressed by replacing or supplementing the gyro propagation with a dynamic one, that is, one that integrates the rigid body equations of motion. By processing quarter-orbit or longer batches, this approach takes advantage of roll-yaw coupling to observe attitude completely without Sun sensor data. Telemetered momentum wheel speeds are used as observations of the unbalanced external torques. GOES-Next provides a unique opportunity to study dynamic attitude propagation. The geosynchronous altitude and adjustable trim tab minimize the external torque and its uncertainty, making long-term dynamic propagation feasible. This paper presents the equations for dynamic propagation, an analysis of the environmental torques, and an estimate of the accuracies obtainable with the proposed method.

1. INTRODUCTION

Accurate attitude determination typically requires a large amount of data taken at different times. This takes advantage of averaging to reduce the effects of sensor noise but requires a means of attitude propagation. Three-axis stabilized spacecraft usually carry gyros that measure how much the spacecraft rotates over short time intervals. For the next series of Geostationary Operational Environmental Satellites (GOES-Next), however, the gyros will be turned off when the spacecraft is on-station, making the usual method of attitude determination impossible.

GOES-Next has Earth and Sun sensors, and when both provide data, it is possible to compute a "single-frame" attitude solution. The Earth sensors provide pitch and roll data; the Sun sensors provide pitch and yaw data. However, the Sun is visible to the Sun sensors for only two-thirds of the day-long orbit, causing an 8-hour period each day when yaw cannot be observed directly. Having an alternative to gyro propagation would make it possible to compute the yaw when the Sun is visible and then predict it for later times when the Sun is out of view. The obvious candidate for this role is the dynamic equation for rigid body rotation, or Euler's equation.

Using Euler's equation to propagate for attitude estimation is not a new idea. In 1976, Lefferts and Markley (Reference 1) and Markley and Wood (Reference 2) applied dynamic propagation to Nimbus-6. The estimator included detailed torque and dynamic modeling and, in addition to solving for attitude and angular velocity, allowed the estimation of torque model parameters. It worked well with simulated data but was unable to duplicate real Nimbus-6 attitude histories. This difficulty seemed due to imperfectly known environmental torques, unmodeled control system activity, and uncertainty about the mass properties of the spacecraft.

Fein (Reference 3) concentrated on the idea of estimating environmental torques from wheel speeds and sensor data. He attributed short-term variations in the speed to the control system and long-term variations to the environmental torques. Based on the knowledge that the attitude remained close to nominal, he was able to model the torques with low-order polynomial functions. Sensor observations served to correct the propagated attitude. Although only time spans up to 22 minutes were considered, agreement with observed attitude histories was good.

Because GOES-Next is at the much higher geosynchronous altitude, environmental torques are expected to be much smaller and correspondingly less uncertain. This should make dynamic propagation more feasible for GOES-Next than for Nimbus-6. Prospects for GOES-Next are further encouraged by its large pitch momentum bias, which stabilizes the spacecraft yaw and roll by keeping the pitch axis aligned with the orbit normal (Reference 4).

This paper describes an attitude estimator that uses Euler's equation, adapts it to the GOES-Next mission, and estimates its accuracy for yaw determination.

2. GOES-NEXT ATTITUDE

The attitude of GOES-Next is defined relative to a rotating reference coordinate system with its z-axis pointing to the center of the Earth; y-axis in the direction of the negative orbit normal; and x-axis oriented so that x, y, and z form a right-handed orthogonal triad. The spacecraft attitude relative to the reference system is defined by a 3-1-2 Euler axis sequence with the three rotation angles referred to as yaw (y), roll (r), and pitch (p) (Reference 5).

The spacecraft roll, pitch, and yaw axes (x, y, and z, respectively) are close to the principal axes of the spacecraft moment-of-inertia tensor. The diagonal components of this tensor in the roll, pitch, yaw frame are I_x = 3364.376 kilogram-meters squared (kg-m^2), I_y = 954.936 kg-m^2, and I_z = 3461.393 kg-m^2, and all of the off-diagonal elements (the products of inertia) are less than 30 kg-m^2 in magnitude.

Estimated attitude uncertainty is due to sensor noise, sensor visibility, and propagation noise. The standard deviation of the sensor noise is a measure of the accuracy of the sensors. Visibility, in this case, involves only Sun visibility since the Earth is assumed to be in view at all times. Propagation noise includes errors in the models of environmental and control torques and unmodeled contributions to these torques.

2.1 SENSORS AND SUN VISIBILITY

GOES-Next has Earth sensors that measure pitch and roll and Sun sensors that measure pitch and yaw; these measurements are telemetered at 0.512-second intervals (Reference 6). Under normal conditions, the Earth sensors provide continuous

measurements. The Sun sensors, however, do not cover the spacecraft z-axis and so do not see the Sun around local midnight.

There are two Earth sensors that scan east-west across the Earth disk and combine their measurements to give pitch and roll. Because of the high altitude, horizon height uncertainty contributes little to sensor error, and the standard deviation of these observations is given as 0.01 degree (1σ). The quantization is also 0.01 degree.

There are two types of Sun sensor. The digital Sun sensor (DSS) is the more accurate of the two, having standard deviation of 0.0042 degree (1σ) and quantization of 0.125 degree. There are also two coarse analog Sun sensor (CASS) systems. These are less accurate, having unspecified noise characteristics and quantization of 0.039 degree. The error for these sensors is on the order of 1 degree on the boresight and increases away from the boresight.

GOES-Next rotates once a day about its y-axis, which is roughly 67 degrees from the ecliptic plane. The percentage of each orbit having Sun coverage is approximately the fraction of the spacecraft x-z plane in the Sun sensor fields of view. As seen from Figure 1, this leaves about one-third of each day without coverage
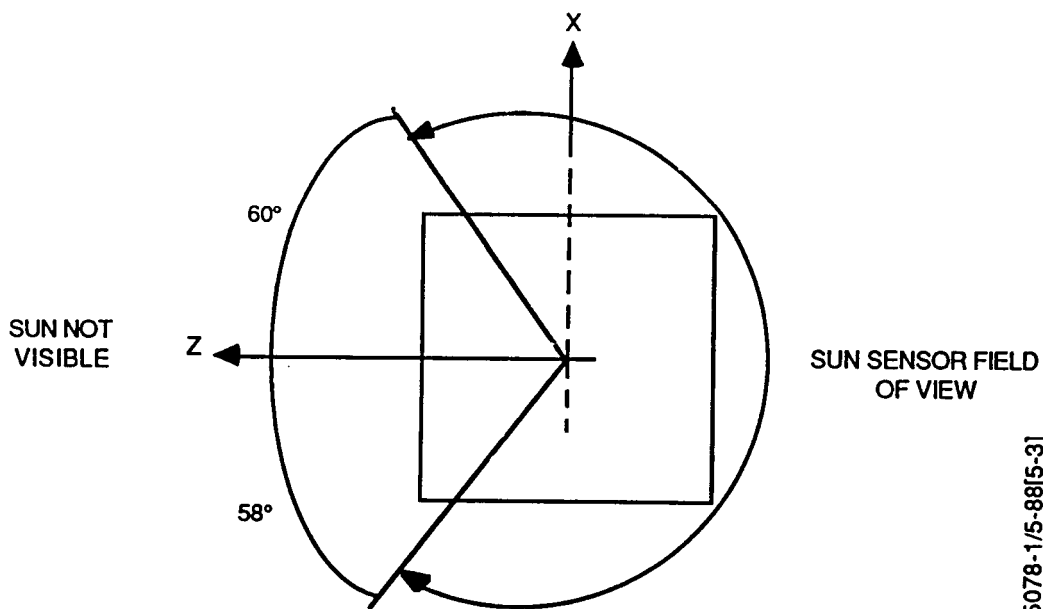

Figure 1. Sun Sensor Field of View

and without yaw observations. It is the more accurate DSS that sees the Sun just before the loss of coverage.

2.2 TORQUES

The torques acting on a spacecraft arise both naturally and from the control system. Natural disturbances include solar radiation, gravity gradient, residual magnetic dipole, and aerodynamic torques. For GOES-Next, which is at geosynchronous altitude, atmospheric torques are negligible. The torques caused by the control system include those due to the magnetic torquers, changing wheel speeds, and thruster activity. Because the thrusters are not expected to be used more than once a day, they are not modeled here.

Solar radiation causes the largest environmental torques on GOES-Next (Reference 7). There is a controllable flap at the end of the solar array that is commanded from the ground to minimize the solar torque. Proper setting of the trim tab can reduce the solar torque to 10^{-7} newton meters (N•m), but the residual torques may be as large as 10^{-5} N•m. The solar torque is approximately a constant scalar times the cross product of the vector from the center of pressure of the solar array to the center of pressure of the solar sail, which is closely aligned with the spacecraft pitch axis, and the Sun-to-spacecraft vector. Thus, the solar torque vector is nearly constant in inertial space and is mostly in the spacecraft roll/yaw plane. In the spacecraft body frame, the largest components of the solar torque are the roll and yaw components, which have sinusoidal time dependence with the orbit period (one sidereal day) with nearly equal magnitudes, and a 90-degree difference in phase. Figure 2 illustrates this dependence of the roll and yaw torques.

Gravity gradient torques depend only on the spacecraft attitude and moment-of-inertia tensor, so they are easily modeled. The largest errors in the gravity gradient torque model come from uncertainty about the inertia tensor for the spacecraft.

Magnetic torques come from residual and control magnetic dipoles (References 8 and 9). The residual dipoles are due to electric currents, magnetized material in the spacecraft, and commanded torquer biases. They are considered to be almost constant in the spacecraft body frame and to have magnitudes of about 8 ampere-meters squared (A-m^2). At geosynchronous altitude, this can produce a torque of at most
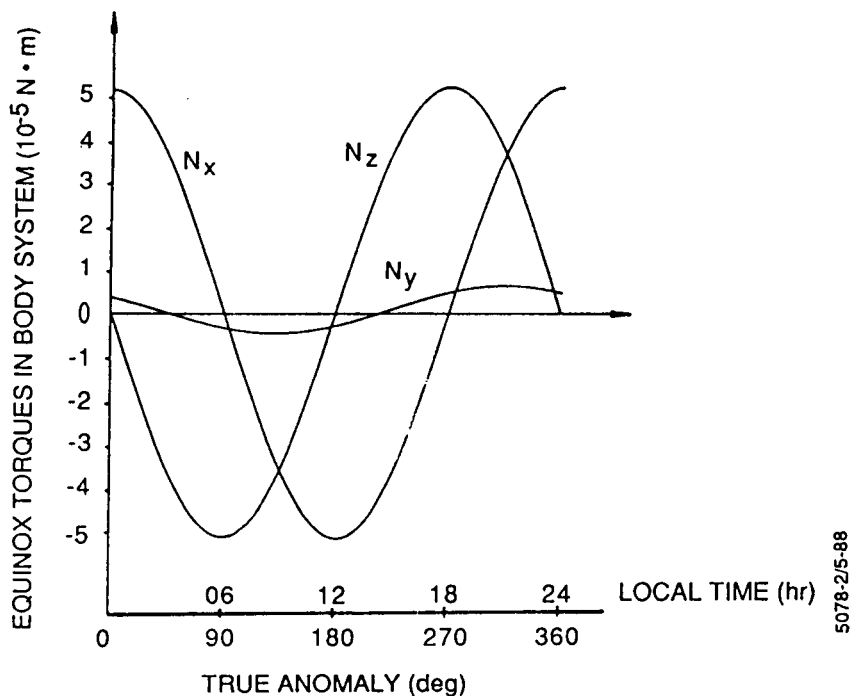
Figure 2. Solar Radiation Torques

10^{-7} N•m. Because of the equatorial orbit of GOES-Next, the Earth's magnetic field is mainly along its pitch axis. Therefore, the torque due to residual dipoles is approximately constant in the body frame. The control dipoles vary slowly over time, producing torques as large as 10^{-6} N•m.

2.3 MOMENTUM WHEELS

GOES-Next is equipped with two momentum wheels with their axes in the pitch-yaw plane, canted at an angle of 1.656 degrees from the pitch axes. These produce a pitch angular momentum bias of

$$H = -I_w(\omega_1 + \omega_2) \cos (1.656^\circ) \tag{1}$$

and a yaw angular momentum of

$$h = I_w(\omega_1 - \omega_2) \sin (1.656^\circ) \tag{2}$$

where ω_1 and ω_2 are the angular velocities of the two wheels in radians per second (rad/sec) and I_w = 0.1082 kg-m^2 is the moment of inertia of each momentum wheel. The nominal on-orbit wheel speeds are 5485 revolutions per minute (rpm) for both wheels, giving H = -124.2 Nms and h = 0. Commanding the wheels in the same direction gives a pitch control torque, and commanding them in opposite directions gives a yaw control torque. The dominant error contribution of the momentum wheels is the torque ripple, which has a maximum spectral density of 6 x 10^{-7} (N•m)^2/hertz (Hz) for each wheel (Reference 10). The momentum wheel speed is measured by a tachometer, sampled at 0.512-second intervals, with a quantization of 0.0163 rpm and a noise level of 0.0978 rpm (3σ) (Reference 11).

Should one momentum wheel fail, the other wheel is operated with a smaller reaction wheel (moment of inertia = 0.008626 kg-m^2) whose axis is along the yaw axis. The speeds of these wheels are nominally set to give a smaller pitch angular momentum bias and zero net angular momentum along the yaw axis, as before. The present analysis is easily extended to this backup situation, but it will not be considered further.

3. DYNAMIC MODEL

For an Earth-pointing spacecraft in a circular orbit, Euler's equation and the kinematic attitude equations can be expressed in terms of roll, pitch, and yaw; the resulting equations can be linearized for small deviations from nominal attitude (e.g., pages 608-610 of Reference 5). The resulting equations for GOES-Next, taking into account the rotation of the reference frame (at one revolution per sidereal day, or ω_0 = 7.29 x 10^{-5} rad/sec) are

$$I_x \ddot{r} - \omega_0 [H - 4(I_y - I_z) \omega_0] r - [H + (I_x - I_y + I_z) \omega_0] \dot{y} = N_x + \omega_0 h \qquad (3a)$$

$$I_y \ddot{p} + 3\omega_0^2 (I_x - I_z) p = N_y - \dot{H} \qquad (3b)$$

$$I_z \ddot{y} - \omega_0 [H - (I_y - I_x) \omega_0] y + [H + (I_x - I_y + I_z) \omega_0] \dot{r} = N_z - N_w \qquad (3c)$$

where r, p, and y are the spacecraft roll, pitch, and yaw in radians; a dot denotes a time derivative; I_x, I_y, and I_z are the diagonal components of the spacecraft moment-of-inertia tensor (the off-diagonal elements have been neglected); H and h are the internal pitch and yaw angular momentum (as defined in Section 2.3); N_x, N_y, and N_z are the external torques on the spacecraft (excluding the gravity gradient torque, which is included on the left-hand sides of the equations); and N_w is the yaw component of the momentum wheel control torque, so that

$$\dot{h} = N_w \tag{4}$$

Equations (3a), (3b), and (3c) exhibit the well-known fact that the spacecraft pitch motion is independent of the coupled roll/yaw motion, to within the accuracy of the linear approximations used to derive these equations. The GOES-Next pitch is well determined by continuous Earth sensor measurements, as discussed in Section 2.1, so this paper will concentrate on the roll/yaw motion.

The numerical values for I_x and I_z given in Section 2 establish the validity of the approximation

$$I_x = I_z = I \equiv (I_x I_z)^{1/2} = 3412.54 \text{ kg-m}^2 \tag{5}$$

The differences of the principal moments of inertia can be ignored in the coefficients containing the bias momentum in Equations (3a) and (3c) since

$$\omega_0 (I_y - I) \simeq 0.0015 \text{ H} \tag{6}$$

With these approximations, Equations (3a) and (3c) can be written

$$\ddot{r} = \omega_0 \omega_n r + (\omega_n + \omega_0) \dot{y} + (N_x + \omega_0 h)/I \tag{7a}$$

$$\ddot{y} = \omega_0 \omega_n y - (\omega_n + \omega_0) \dot{r} + (N_z - N_w)/I \tag{7b}$$

where the nutation frequency ω_n is given by

$$\omega_n = H/I = 0.0364 \text{ rad/sec} \tag{8}$$

437

This corresponds to a nutation period of 173 seconds.

Precise attitude estimation will require simultaneous estimation of unmodeled torques, in view of the difficulty of accurately modeling the disturbance and control torques. As discussed in Section 2.2, the principal torque modeling errors have both a constant term $\bar{N}_c$ and a sinusoidal term $\bar{N}_p$ with angular frequency ω_0. Thus, the torques are

$$N_x = N_x^* + N_{cx} + N_{px} + w_x \tag{9a}$$

$$N_z = N_z^* + N_{cz} + N_{pz} + w_z \tag{9b}$$

$$N_w = N_w^* + w_w \tag{9c}$$

where N_x^*, N_z^*, and N_w^* are the modeled roll, yaw, and wheel torques, respectively, and w_x, w_z, and w_w are independent white noise processes. The estimated values of $\bar{N}_c$ and $\bar{N}_p$ will include all the unmodeled torques with the prescribed time dependence.

A nine-component state vector containing all the parameters to be estimated is

$$\bar{x} \equiv [r, \dot{r}/\omega_n, y, \dot{y}/\omega_n, h, N_{px}, N_{pz}, N_{cx}, N_{cz}]^T \tag{10}$$

where superscript T denotes the matrix transpose. For GOES-Next, variations in H, and therefore in ω_n, are very small and can be ignored. Then, combining Equations (4), (7), (9), and (10) with the assumed sinusoidal dependence of $\bar{N}_p$ gives the dynamic equation

$$\dot{\bar{x}} = F\,\bar{x} + \bar{u} + \bar{w} \tag{11a}$$

where

$$F = \begin{bmatrix} A & \vdots & B \\ -- & \vdots & -- \\ 0 & \vdots & C \end{bmatrix} \tag{11b}$$

438

with

$$
A = \begin{bmatrix}
0 & \omega_n & 0 & 0 \\
\omega_o & 0 & 0 & \omega_n + \omega_o \\
0 & 0 & 0 & \omega_n \\
0 & -(\omega_n + \omega_o) & \omega_o & 0
\end{bmatrix}
\tag{11c}
$$

$$
B = \frac{1}{H} \begin{bmatrix}
0 & 0 & 0 & 0 & 0 \\
\omega_o & 1 & 0 & 1 & 0 \\
0 & 0 & 0 & 0 & 0 \\
0 & 0 & 1 & 0 & 1
\end{bmatrix}
\tag{11d}
$$

$$
C = \omega_o \begin{bmatrix}
0 & 0 & 0 & 0 & 0 \\
0 & 0 & 1 & 0 & 0 \\
0 & -1 & 0 & 0 & 0 \\
0 & 0 & 0 & 0 & 0 \\
0 & 0 & 0 & 0 & 0
\end{bmatrix}
\tag{11e}
$$

and O is a 5-by-4 matrix of zeros.

The nine-component vectors $\bar{u}$ and $\bar{w}$ are given by

$$
\bar{u} = [0, N_x^*/H, 0, (N_z^* - N_w^*)/H, N_w^*, 0, 0, 0, 0]^T
\tag{12a}
$$

and

$$
\bar{w} = [0, w_x/H, 0, (w_z - w_w)/H, w_w, w_{px}, w_{pz}, w_{cx}, w_{cz}]^T
\tag{12b}
$$

where w_{px}, w_{pz}, w_{cx}, and w_{cz} are independent (of each other and of w_x, w_z, and w_w) random noise processes. If w_{cx} and w_{cz} are not zero, $\bar{N}_c$ will not be truly constant but will behave as a random walk. Nonzero w_{px} and w_{pz} will give random walk dependence to the phase and amplitude of $\bar{N}_p$.

439

Equation (11a) has the formal solution

$$\bar{x}(t) = \Phi(t, t_0) \bar{x}(t_0) + \int_{t_0}^{t} \Phi(t, t')[\bar{u}(t') + \bar{w}(t')] \, dt' \tag{13}$$

where the state transition matrix $\Phi(t, t_0)$ is a solution of

$$\dot{\Phi}(t, t_0) = F \, \Phi(t, t_0) \tag{14a}$$

with the initial condition

$$\Phi(t_0, t_0) = I_9 \equiv \text{the } 9 \times 9 \text{ identity matrix} \tag{14b}$$

To avoid confusion, capital I denoting an identity matrix will always have a numerical subscript, and capital I denoting moment of inertia will have either a literal subscript or no subscript. The state transition matrix has a partitioning similar to Equation (11b):

$$\Phi(t, t_0) = \begin{bmatrix} \phi(t, t_0) & \vdots & \theta(t, t_0) \\ ---- & \vdots & ---- \\ 0 & \vdots & \psi(t, t_0) \end{bmatrix} \tag{15}$$

Substituting Equation (15) into Equations (14a) and (14b) gives

$$\dot{\phi}(t, t_0) = A \, \phi(t, t_0) \qquad \text{with } \phi(t_0, t_0) = I_4 \tag{16a}$$

$$\dot{\psi}(t, t_0) = C \, \psi(t, t_0) \qquad \text{with } \psi(t_0, t_0) = I_5 \tag{16b}$$

and

$$\dot{\theta}(t, t_0) = A \, \theta(t, t_0) + B \, \psi(t, t_0) \qquad \text{with } \theta(t_0, t_0) = 0 \tag{16c}$$

440

The solution of Equation (16c) is

$$\Theta(t, t_0) = \int_{t_0}^{t} \phi(t, t') B \psi(t', t_0) \, dt' \tag{17}$$

so $\Theta(t, t_0)$ is determined when $\phi(t, t_0)$ and $\psi(t, t_0)$ are determined. The solution of Equation (16b) is easily seen to be

$$\psi(t, t_0) = \begin{bmatrix} 1 & 0 & 0 & 0 & 0 \\ 0 & c_0 & s_0 & 0 & 0 \\ 0 & -s_0 & c_0 & 0 & 0 \\ 0 & 0 & 0 & 1 & 0 \\ 0 & 0 & 0 & 0 & 1 \end{bmatrix} \tag{18}$$

where

$$c_0 \equiv \cos \omega_0 (t - t_0) \tag{19a}$$

and

$$s_0 \equiv \sin \omega_0 (t - t_0) \tag{19b}$$

It is thus seen that the structure of the matrix C gives the desired sinusoidal dependence of $\overline{N}_p$.

Equation (16a) is more difficult to solve. Since A is constant,

$$\phi(t, t_0) = \exp [A(t - t_0)] \tag{20}$$

The characteristic equation of A is

$$0 = \det [A - \lambda I_4] = \left(\lambda^2 + \omega_0^2\right)\left(\lambda^2 + \omega_n^2\right) \tag{21}$$

441

so the eigenvalues of this matrix are $\pm i\omega_0$ and $\pm i\omega_n$. With Equation (20), this shows that $\phi(t, t_0)$ comprises sinusoidal terms with angular frequencies ω_0 and ω_n. This is the justification for referring to ω_n as the nutation frequency. Note that the characteristic equation is intractable without the assumptions leading from Equations (3a) and (3c) to Equations (7a) and (7b). With the periodic nature of $\phi(t, t_0)$ known, it is not too difficult to show that the solution of Equation (16a) is

$$\phi(t, t_0) = \phi_0(t, t_0) + \phi_n(t, t_0) \tag{22a}$$

where

$$\phi_0(t, t_0) = \frac{1}{\omega_n - \omega_0} \begin{bmatrix} \omega_n c_0 & -\omega_n s_0 & \omega_n s_0 & \omega_n c_0 \\ -\omega_0 s_0 & -\omega_0 c_0 & \omega_0 c_0 & -\omega_0 s_0 \\ -\omega_n s_0 & -\omega_n c_0 & \omega_n c_0 & -\omega_n s_0 \\ -\omega_0 c_0 & \omega_0 s_0 & -\omega_0 s_0 & -\omega_0 c_0 \end{bmatrix} \tag{22b}$$

with c_0 and s_0 defined by Equations (19a) and (19b), and

$$\phi_n(t, t_0) = \frac{1}{\omega_n - \omega_0} \begin{bmatrix} -\omega_0 c_n & \omega_n s_n & -\omega_0 s_n & -\omega_n c_n \\ \omega_0 s_n & \omega_n c_n & -\omega_0 c_n & \omega_n s_n \\ \omega_0 s_n & \omega_n c_n & -\omega_0 c_n & \omega_n s_n \\ \omega_0 c_n & -\omega_n s_n & \omega_0 s_n & \omega_n c_n \end{bmatrix} \tag{22c}$$

with

$$c_n \equiv \cos \omega_n(t - t_0) \tag{23a}$$

and

$$s_n \equiv \sin \omega_n(t - t_0) \tag{23b}$$

Substituting Equations (18) and (22a), (22b), and (22c) into Equation (17) gives integrals that are convolutions of trigonometric functions and can be evaluated without too much difficulty. The terms in $\Theta(t, t_0)$ have only six kinds of time dependence: $1-c_n$, s_n, $1-c_0$, s_0, $\omega_0(t - t_0)c_0$, and $\omega_0(t - t_0)s_0$.

4. OBSERVABILITY

Before proceeding to detailed treatment of the attitude estimation algorithms, it is useful to establish that the attitude state defined in Section 3 is observable. To discuss observability in a more general sense, consider an n-dimensional state vector and an m-dimensional vector of measurements of $\bar{x}$:

$$\bar{g} = G\bar{x} \tag{24}$$

where G is an m-by-n matrix. Then the state is observable if and only if the nm-by-n observability matrix

$$M \equiv \begin{bmatrix} G \\ GF \\ GF^2 \\ \cdot \\ \cdot \\ \cdot \\ GF^{n-1} \end{bmatrix} \tag{25}$$

has full rank n, where F is the dynamic matrix defined by Equation (11a) for the n-component state $\bar{x}$.

Consider first the full nine-component state, with F given by Equations (11b) through (11e). If roll, yaw, and wheel tachometer measurements are available, m = 3 and

$$G = \begin{bmatrix} 1 & 0 & 0 & 0 & 0 & 0 & 0 & 0 & 0 \\ 0 & 0 & 1 & 0 & 0 & 0 & 0 & 0 & 0 \\ 0 & 0 & 0 & 0 & 1 & 0 & 0 & 0 & 0 \end{bmatrix} \tag{26}$$

443

A computation of M shows that the state is observable in this case; in fact, computing G, GF, GF^2, and GF^3 achieves full rank. Thus, the roll/yaw attitude, attitude rates, wheel speed, and torques are all observable with roll, yaw, and tachometer measurements.

The observability when yaw measurements are not available is also of interest, as discussed in Section 2.1. With only roll and tachometer measurements, m = 2 and

$$
G'' = \begin{bmatrix} 1 & 0 & 0 & 0 & 0 & 0 & 0 & 0 & 0 \\ 0 & 0 & 0 & 0 & 1 & 0 & 0 & 0 & 0 \end{bmatrix} \tag{27}
$$

The observability matrix computed with this has rank eight, so the nine-component state is not observable.

To ascertain which parameters are observable and which are not, consider the eight-component state vector obtained by deleting the constant yaw torque from $\bar{x}$:

$$
\bar{x}' \equiv [r, \dot{r}/\omega_n, y, \dot{y}/\omega_n, h, N_{px}, N_{pz}, N_{cx}]^T \tag{28}
$$

This obeys the state equation

$$
\dot{\bar{x}}' = F' \bar{x}' + \bar{u}' + \bar{w}' \tag{29a}
$$

where

$$
F = \begin{bmatrix} A & \vdots & B' \\ -- & \vdots & -- \\ 0 & \vdots & C' \end{bmatrix} \tag{29b}
$$

with

$$
B' = \frac{1}{H} \begin{bmatrix} 0 & 0 & 0 & 0 \\ \omega_0 & 1 & 0 & 1 \\ 0 & 0 & 0 & 0 \\ 0 & 0 & 1 & 0 \end{bmatrix} \tag{29c}
$$

and

$$
C' = \omega_0 \begin{bmatrix} 0 & 0 & 0 & 0 \\ 0 & 0 & 1 & 0 \\ 0 & -1 & 0 & 0 \\ 0 & 0 & 0 & 0 \end{bmatrix} \tag{29d}
$$

With only roll and tachometer measurements

$$
G' = \begin{bmatrix} 1 & 0 & 0 & 0 & 0 & 0 & 0 & 0 \\ 0 & 0 & 0 & 0 & 1 & 0 & 0 & 0 \end{bmatrix} \tag{30}
$$

Forming the observability matrix from products $G'(F')^k$ for power k up to six gives full rank, establishing that the attitude, attitude rates, wheel speed, periodic torque and constant roll torque are observable with only roll and tachometer measurements. It is more difficult to observe the reduced state without yaw measurements than to observe the full state using yaw measurements along with the roll and tachometer measurements, as indicated by the need for higher powers of F in the former case.

The preceding computations establish that the full nine-component state is observable with roll, yaw, and tachometer measurements, but the constant yaw torque is unobservable in the absence of yaw measurements, the other eight components of the state remaining observable from roll and tachometer measurements. This indicates that the constant yaw torque must be estimated during periods with yaw measurements, and that the errors in this torque must not grow too rapidly in periods without Sun sensor visibility. This is equivalent to the assumption that the error source w_{cz} is small.

5. KALMAN FILTER

In principle, the GOES-Next attitude estimation could be carried out using either a batch least-squares estimator or a Kalman filter. The Kalman filter is preferred because it is more straightforward to account for process noise with this method. The observability analysis of Section 4 shows that yaw data are needed to estimate

the constant yaw torque. Thus, a batch estimator must use at least one-third of an orbit, or 8 hours, of data to estimate the GOES-Next yaw across the period of yaw data outage. It is very likely that the dynamic models are not accurate enough to propagate across this interval without accounting for process noise. Thus, only the Kalman filter will be considered in this paper.

The Kalman filter propagates estimates of the state $\hat{x}_{k-1}(+)$ and covariance matrix $P_{k-1}(+)$ immediately after the $(k-1)^{st}$ measurement to the time t_k of the kth measurement by means of the following equations:

$$\hat{x}_k(-) = \Phi(t_k, t_{k-1}) \, \hat{x}_{k-1}(+) + \int_{t_{k-1}}^{t_k} \Phi(t_k, t') \, \bar{u}(t') \, dt' \tag{31}$$

and

$$P_k(-) = \Phi(t_k, t_{k-1}) \, P_{k-1}(+) \, \Phi^T(t_k, t_{k-1}) \tag{32}$$

$$+ \int_{t_{k-1}}^{t_k} \Phi(t_k, t') \, Q \, \Phi^T(t_k, t') \, dt'$$

where the transition matrix Φ is given by Equation (15) and the process noise spectral density matrix Q is defined by

$$E[\bar{w}(t) \, \bar{w}^T(t')] = Q \, \delta(t - t') \tag{33}$$

E denotes the expectation value, $\bar{w}$ is defined by Equation (12b), and $\delta(t - t')$ denotes the Dirac delta (unit impulse) function. Equation (31) is simply Equation (13) without the unknown process noise term, $\bar{w}$. The explicit form for the process noise spectral density matrix is

$$Q = \begin{bmatrix} Q_{5x5} & \vdots & 0 \\ - - - & \vdots & - - - \\ 0 & \vdots & Q_{4x4} \end{bmatrix} \tag{34a}$$

with

$$Q_{5x5} = \begin{bmatrix} 0 & 0 & 0 & 0 & 0 \\ 0 & q_x/H^2 & 0 & 0 & 0 \\ 0 & 0 & 0 & 0 & 0 \\ 0 & 0 & 0 & (q_z + q_w)/H^2 & -q_w/H \\ 0 & 0 & 0 & -q_w/H & q_w \end{bmatrix} \tag{34b}$$

and

$$Q_{4x4} = \text{diag} \, [q_{px}, \, q_{pz}, \, q_{cx}, \, q_{cz}] \tag{34c}$$

where the latter notation means that Q_{4x4} is a diagonal matrix with the indicated arguments as the elements on the main diagonal. The scalar spectral density q_x is defined by

$$E[w_x(t) \, w_x(t')] = q_x \delta(t - t') \tag{35}$$

and similar relations hold for q_z, q_w, q_{px}, q_{pz}, q_{cx}, and q_{cz}. The results of Section 3 allow closed form evaluation of the integral in Equation (32), giving a very efficient means of covariance propagation.

When a measurement is processed, the state estimate and covariance matrix are updated as follows:

$$\hat{x}_k(+) = \hat{x}_k(-) + K_k[\bar{g}_k - G_k\hat{x}_k(-)] \tag{36}$$

and

$$P_k(+) = (I_9 - K_kG_k) \, P_k(-) \, (I_9 - K_kG_k)^T + K_kR_kK_k^T \tag{37}$$

where $\bar{g}_k$ is the vector of measured values at time t_k, G_k is the matrix relating the measurement to the state as in Section 4, R_k is the measurement covariance and K_k is the Kalman gain:

$$K_k = P_k(-) \, G_k^T \left[G_kP_k(-)G_k^T + R_k\right]^{-1} \tag{38}$$

If the attitude estimates are not needed in near-real time, an optimal filter-smoother may be preferable to a Kalman filter (Reference 12), but that option will not be considered in this paper.

6. ACCURACY ESTIMATES

In the absence of detailed simulations, quantitative estimates of the accuracy attainable with the proposed estimation procedure require the use of approximate models. This paper will consider the accuracy during periods when no yaw measurements are available, because these periods test the attitude estimation process more severely than periods containing yaw data. The observability analysis of Section 4 shows that the external torques are not completely observable without yaw data; the model will therefore be simplified here by eliminating the torques from the state vector. The remaining five-component state has an estimation error represented by a 5-by-5 covariance matrix, and the accuracy estimates will be obtained by computing an approximation to this matrix. The computation can be further simplified by averaging the covariance propagation Equation (32) over a nutation period, using the results of Section 3 for the transition matrix, and

then considering the limit at which the orbit rate is negligible compared to the nutation rate. This permits the deletion of the roll rate and yaw rate from the state, resulting in an effective 3-by-3 covariance matrix. The steady-state covariance can then be found by solving a quartic equation, which is possible in principle but inconvenient in practice. However, the simplified approach presented below gives equivalent results for the steady-state covariance.

The validity of the approximate steady-state covariance analysis rests on two quantitative aspects of the GOES-Next attitude determination. First, the orbit rate is much less than the nutation rate, by a factor of 2×10^{-3}. Second, the wheel tachometer measurements are so accurate that the yaw component of the internal angular momentum, which is a component of the state vector, is essentially determined by tachometer measurements alone; the correlation between its errors and the attitude errors is thus effectively zero.

Consider the dynamic Equations (7a) and (7b) in the limit that ω_n becomes infinite. The resulting equations will describe motion on time scales large compared to the nutation period, with nutation averaged out. The second derivative terms in Equations (7a) and (7b) are seen to be negligible if nutation is ignored. The factor $1/I$ is replaced by ω_n/H using Equation (8), and H is held at its physical value as ω_n is taken to infinity. This means that the rotational inertia of the spacecraft body is dominated by the bias angular momentum on time scales larger than the nutation period. The limits of Equations (7a) and (7b) are

$$0 = \omega_0 r + \dot{y} + (N_x + \omega_0 h)/H \tag{39a}$$

$$0 = \omega_0 y - \dot{r} + (N_z - N_w)/H \tag{39b}$$

The two-component state

$$\tilde{x} \equiv [r + h/H, \ y]^T \tag{40}$$

obeys the dynamic equation

$$\dot{\tilde{x}} = \tilde{F} \tilde{x} + \tilde{u} + \tilde{w} \tag{41a}$$

449

with

$$\tilde{F} = \omega_0 \begin{bmatrix} 0 & 1 \\ -1 & 0 \end{bmatrix} \tag{41b}$$

$$\tilde{u} = H^{-1} \begin{bmatrix} N_z^*, & -N_x^* \end{bmatrix}^T \tag{42a}$$

and

$$\tilde{w} = H^{-1} \begin{bmatrix} w_z, & -w_x \end{bmatrix}^T \tag{42b}$$

Equation (4) was used in deriving these equations. With the assumption that q_x and q_z, defined in Equation (35), are equal, the process noise spectral density matrix, defined by an equation analogous to Equation (33), is

$$\tilde{Q} = (q/H^2) I_2 \tag{43}$$

where q denotes the common value of q_x and q_z.

In this derivation, q is the spectral density of the process noise representing unmodeled external torques. The more rigorous method of averaging over a nutation period, as discussed at the beginning of this section, shows that a contribution $1/2 \, q_w$ from the momentum wheels should be added to q, the factor of 1/2 arising from the time average of $\sin^2 \omega_n t$ and $\cos^2 \omega_n t$. Since q_w arises from torque ripple, as discussed in Section 2, its numerical value can be estimated as

$$q_w = 2(\sin 1.656^\circ)^2 (6 \times 10^{-7}/2\pi)(N \cdot m)^2 \, s = 1.3 \times 10^{-10} (N \cdot m)^2 \, s \tag{44}$$

where the factor of 2 appears because two wheels contribute to h, and 2π is the conversion from hertz to radians per second. The environmental torque errors are not well approximated by a white noise process, but the spectral density of these

errors can be estimated by multiplying the mean square torque errors by a correlation time. The maximum expected torque errors are about 10 percent of the amplitude of equinox torques shown in Figure 2. The quarter-orbit period, which also gives the filter memory span required to estimate yaw, is a reasonable estimate of the correlation time. Thus, an upper limit of the spectral density of external torques is

$$q = \left(5 \times 10^{-6} \text{ N} \cdot \text{m}\right)^2 (21541 \text{ s}) = 5.4 \times 10^{-7} \text{ (N} \cdot \text{m)}^2 \text{ s} \qquad (45)$$

The wheel torque ripple spectral density, q_w, is negligible compared to this. The speed of each momentum wheel is measured at 0.512-second intervals with error variance:

$$R_{tach} = [(0.0163)^2/12 + (0.0978/3)^2](2\pi/60)^2 \text{(rad/s)}^2 = 1.2 \times 10^{-5} \text{ (rad/s)}^2 \qquad (46)$$

where the factor of 12 converts quantization error to variance and $2\pi/60$ converts revolutions per minute to radians per second. The roll is also measured at 0.512-second intervals with error variance:

$$R_{roll} = [(0.01)^2/12 + (0.01)^2](\pi/180)^2 \text{ rad}^2 = 3.3 \times 10^{-8} \text{ rad}^2 \qquad (47)$$

where $\pi/180$ converts degrees to radians. These measurements can be combined to give a measurement of the first component of $\tilde{x}$ with error variance

$$R_k = R_{roll} + 2 \left(I_w \sin 1.656^\circ/H\right)^2 R_{tach} \simeq R_{roll} \qquad (48)$$

since the tachometer errors are negligible.

Since the measurement interval Δt is much less than the nutation period, which has already been neglected in deriving Equation (41a), the measurements can be treated as continuous rather than discrete. This leads to a first-order differential equation for the covariance (Reference 12):

$$\dot{\tilde{P}} = \tilde{F}\tilde{P} + \tilde{P}\tilde{F}^T + \tilde{Q} - \tilde{P}\tilde{G}^T R^{-1} \tilde{G}\tilde{P} \tag{49}$$

where

$$\tilde{G} = [1 \ 0]^T \tag{50}$$

and

$$R = R_k \Delta t = 1.7 \times 10^{-8} \ rad^2 s \tag{51}$$

Writing

$$\tilde{P} = \begin{bmatrix} p_{11} & p_{12} \\ p_{12} & p_{22} \end{bmatrix} \tag{52}$$

and using Equations (41b) and (43) gives the three scalar equations:

$$\dot{p}_{11} = 2 \, \omega_o p_{12} + q/H^2 - p_{11}^2/R \tag{53a}$$

$$\dot{p}_{22} = -2 \, \omega_o p_{12} + q/H^2 - p_{12}^2/R \tag{53b}$$

$$\dot{p}_{12} = \omega_o(p_{22} - p_{11}) - p_{11} \, p_{12}/R \tag{53c}$$

Solving Equations (53a), (53b), and (53c) for the covariance for which the time derivatives vanish gives the following steady-state covariance:

$$P_{11} = \omega_0 R[(\alpha + 3)(\alpha - 1)]^{1/2} \qquad (54a)$$

$$P_{22} = \omega_0 R \, \alpha[(\alpha + 3)(\alpha - 1)]^{1/2} \qquad (54b)$$

$$P_{12} = \omega_0 R(\alpha - 1) \qquad (54c)$$

where

$$\alpha \equiv \left[1 + q/\left(\omega_0^2 H^2 R\right) \right]^{1/2} \qquad (54d)$$

Taking α equal to the negative of the square root in Equation (54d) also gives a steady-state solution, but this is unacceptable because it gives a negative value for P_{22}, which must be nonnegative.

The principal quantity of interest for this analysis is the variance of the yaw estimate, or P_{22}. For GOES-Next, $q/(\omega_0^2 H^2 R) = 3.9 \times 10^5 \gg 1$, so to an excellent approximation:

$$P_{22} \simeq \omega_0 R \alpha^2 \simeq q/\left(\omega_0 H^2\right) \qquad (55)$$

It is remarkable that the yaw variance is independent of the measurement error R in this limit. Equation (55) provides a general parameterization of the yaw accuracy as a function of the torque modeling errors. Inserting the GOES-Next values for the parameters gives

$$\sigma_{yaw} = (P_{22})^{1/2} \simeq 6.9 \times 10^{-4} \text{ rad} = 0.040 \text{ deg} \qquad (56)$$

This is very close to the performance expected by the spacecraft contractor (Reference 10).

7. CONCLUSIONS

Dynamic propagation promises to be a valuable complement to gyro propagation for GOES-Next, permitting observation of yaw during Sun sensor data gaps and estimation of environmental torques for setting the trim tab. Provided the attitude remains close to Earth pointing, the propagation equations are nearly linear. The added assumption that the body angular momentum is much smaller than that of the momentum wheels allows closed-form solution of those equations. The solution has terms that vary at the orbital rate and at the much higher nutation rate. Neglecting errors with greater than the nutation frequency allows closed-form expressions for the yaw accuracy, also.

Error enters the propagation through imperfectly modeled environmental torques, control torques that are ignored because of lack of information, and random fluctuations in the wheel-bearing torque. The largest sources of error are expected to be the solar torque modeling and the neglected magnetic control torques. The stabilizing pitch momentum bias, the accurate wheel tachometer data, and the relatively small torques at geosynchronous altitude permit propagation in the presence of these errors.

Since the error propagation equations are linear, the Kalman filter proposed here is also linear and should be easier to develop than a general extended Kalman filter. With the transition matrices calculated in closed form, the filter should also be efficient to operate. In practice, this filter would process full orbits of data to estimate torque parameters and propagate the yaw during Sunless periods. The process and sensor noise levels expected for GOES-Next yield an estimated yaw accuracy of 0.040 deg following the gap in Sun coverage. This number is consistent with manufacturer estimates of yaw drift over that period. Successfully applying dynamic propagation to GOES-Next operations support would break new ground for the Flight Dynamics Division of the Goddard Space Flight Center and would provide a much needed backup to the usual gyro propagation.

REFERENCES

1. E. J. Lefferts and F. L. Markley, "Dynamic Modeling for Attitude Determination," AIAA Guidance and Control Conference, San Diego, California, August 1976, paper no. 76-1910

2. Computer Sciences Corporation, CSC/TM-76/6235, Nimbus-G Attitude Determination Feasibility Study Utilizing the Attitude Dynamics Generator (ADGEN), F. L. Markley and J. W. Wood, December 1976

3. --, CSC/TM-77/6115, Evaluation of Wheel Rate Data for LANDSAT Attitude Modeling, J. Fein, April 1977

4. Ford Aerospace and Communications Corporation, DRL 302-01, GOES IJK/LM Attitude/Orbit Control Analysis, January 15, 1987

5. J. R. Wertz, ed., Spacecraft Attitude Determination and Control. D. Reidel: Dordrecht, Holland, 1978

6. Ford Aerospace and Communications Corporation, DRL 300-03, GOES IJK/LM Fields of View Analysis, December 17, 1986

7. Computer Sciences Corporation, "Notes on GOES-Next Solar Torque Analysis," unpublished, J. Rowe, October 1977

8. Ford Aerospace and Communications Corporation, PCC-TM-0733, ODC-86-053, "Compensation of S/C Magnetic Dipole Using the Magnetic Torquers," C. Weyandt, November 11, 1986

9. --, PCC-TM-0966, ODC-87-059, "Need for Magnetic Torquers," C. Weyandt, February 18, 1987

10. --, "Dynamics and Controls Analysis CDR Data Package," Book 2, March 8-9, 1988

11. T. Kailath, Linear Systems. Prentice-Hall: Englewood Cliffs, New Jersey, 1980

12. A. Gelb, ed., Applied Optional Estimation. M.I.T. Press: Cambridge, Massachusetts, 1974